

Color Shift Model-Based Segmentation and Fusion for Digital Autofocusing

Vivek Maik

Image Processing and Intelligent Systems Lab, Graduate School of Advanced Imaging Science, Multimedia and Film, Chung Ang University, Seoul 156-756, South Korea
E-mail: vivek5681@wm.cau.ac.kr

Dohee Cho

Digital/Scientific Imaging Lab, Graduate School of Advanced Imaging Science, Multimedia and Film, Chung Ang University, Seoul 156-756, South Korea

Jeongho Shin

Department of Web Information Engineering, Hankyong National University, Anseong 456-749, South Korea

Donghwan Har

Digital/Scientific Imaging Lab, Graduate School of Advanced Imaging Science, Multimedia and Film, Chung Ang University, Seoul 156-756, South Korea

Joonki Paik

Image Processing and Intelligent Systems Lab, Graduate School of Advanced Imaging Science, Multimedia and Film, Chung Ang University, Seoul 156-756, South Korea

Abstract. *This paper proposes a novel color shift model-based segmentation and fusion algorithm for digital autofocusing of color images. The source images are obtained using new multiple filter-aperture configurations. We shift color channels to change the focal point of the given image at different locations. For each respective location we then select the optimal focus information and, finally, use soft decision fusion and blending (SDFB) to obtain fully-focused images. The proposed autofocusing algorithm consists of: (i) color channel shifting and alignment for varying focal positions; (ii) optimal focus region selection and segmentation using sum modified Laplacian (SML); and (iii) SDFB, which enables smooth transition across region boundaries. By utilizing segmented images for different focal point locations, the SDFB algorithm can combine images with multiple, out-of-focus objects. Experimental results show performance and feasibility of the proposed algorithm for autofocusing images with one or more differently out-of-focus objects. © 2007 Society for Imaging Science and Technology. [DOI: 10.2352/J.ImagingSci.Technol.(2007)51:4(368)]*

INTRODUCTION

Demand for digital autofocusing techniques is rapidly increasing in many visual applications, such as camcorders, digital cameras, and video surveillance systems. Until now, most focusing efforts have been put on gray scale images. Even with specialized color processing techniques, each color channel is processed independently for autofocusing applications. In this paper, a novel autofocusing algorithm utiliz-

ing color shift property is proposed, which can restore an image with multiple, differently focused objects. We propose a new filter-aperture (FA) model for autofocusing color images. The proposed method overcomes the fusion with multiple source images as it uses a single input image. The FA model separates and distributes the out-of-focusing blur into different color channels. The multiple FA models also make it possible to generate as many source images as necessary for fusion-based autofocusing. Multiple focal points are spotted on the image and color channel shifting aligns each channel with the respective focal point. For each alignment the sum modified Laplacian (SML) operator is used to obtain a numerical measure indicating the degree of focus of that image. The in-focus pixels are selected and combined at each process using soft decision fusion and blending (SDFB) to produce the in-focus image with maximum focus metric. The SML operator can also be used to estimate a number of focal points starting from the minimum degree of focus in the input image. The proposed algorithm does not use any restoration filter, which usually results in undesired artifacts, such as ringing, reblurring, and noise clustering.

The rest of the paper is organized as follows. The following section summarizes existing techniques, and presents the major contribution of the proposed work. The section titled “Multiple FA model” gives a detailed description of the multiple FA method and “Digital Autofocusing Algorithm” describes the proposed autofocusing algorithm. “Experi-

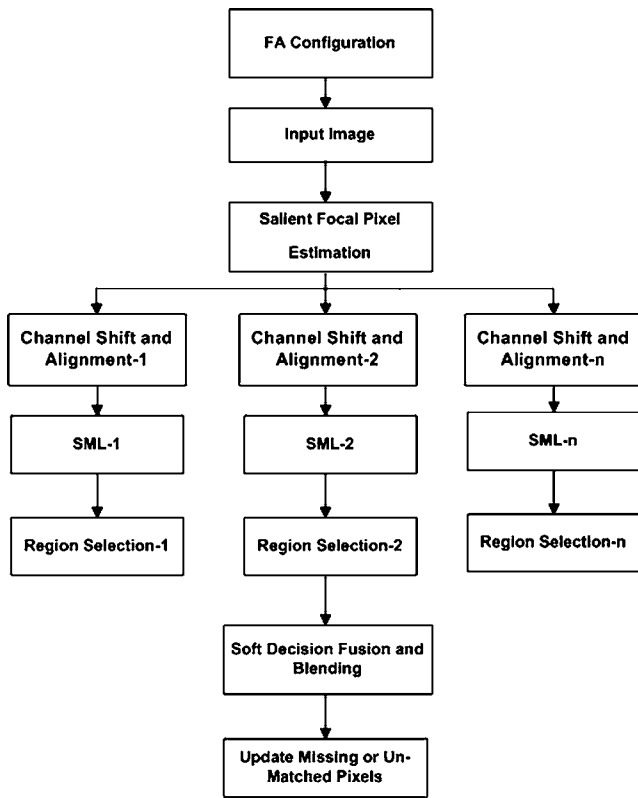


Figure 1. Block diagram of the proposed algorithm.

mental Results” shows the simulation results and comparisons with existing methods. Finally, we have the concluding remarks.

EXISTING STATE-OF-THE-ART AUTOFOCUSING METHODS

FA Model

The conventional photo sensor array uses micro lenses in front of every pixel to concentrate light onto the photosen-

sitive region.¹ In this paper, we can interpret the optical design in a gradual step that we are able to make the multiple detectors beneath the each micro lens, instead of multiple arrays of detectors. The artificial compound eye sensor (insect eyes) is composed of a micro lens array and a photo sensor.² However, the imaging quality of these optical designs is fundamentally inferior to a camera system with a large single lens; the resolution of these small lens arrays is severely limited by diffraction. The “wave front coding” system³ is similar to the proposed system (see Figure 1) in that it provides a way to decouple the trade-off between aperture size and depth of field, but their design is very different. Rather than collecting and resorting rays of light, they use aspheric lenses that produce images with a depth-independent blur. Deconvolution of these images retrieves image details at all depths as shown in Figure 2.

Autofocusing Methods

The traditional autofocusing system in a camera usually consists of two different modules: analysis and control. The analysis module estimates a degree-of-focus of an image projected onto the image plane. The control module performs focusing functions by moving the lens assembly to the optimal focusing position according to the degree-of-focus information estimated in the analysis module. There are five different focusing techniques, such as manual focusing (MF), infrared autofocusing (IRAF), through-the-lens autofocusing (TTLAF), semi-digital autofocusing (SDAF), and fully digital autofocusing (FDAF).⁴⁻⁷ Table I briefly summarizes and compares those techniques.

The FDAF systems usually involve restoration and fusion methods in the control module which operates using prior information like point spread function (PSF), gradients, multiple source inputs, etc. to obtain the details about out-of-focus blur in images. Image fusion-based autofocus-

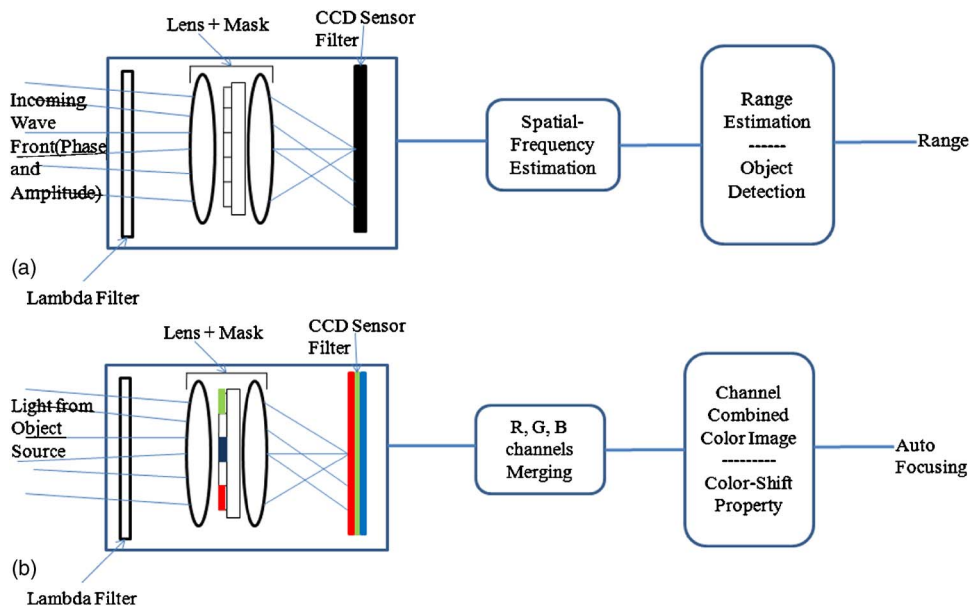
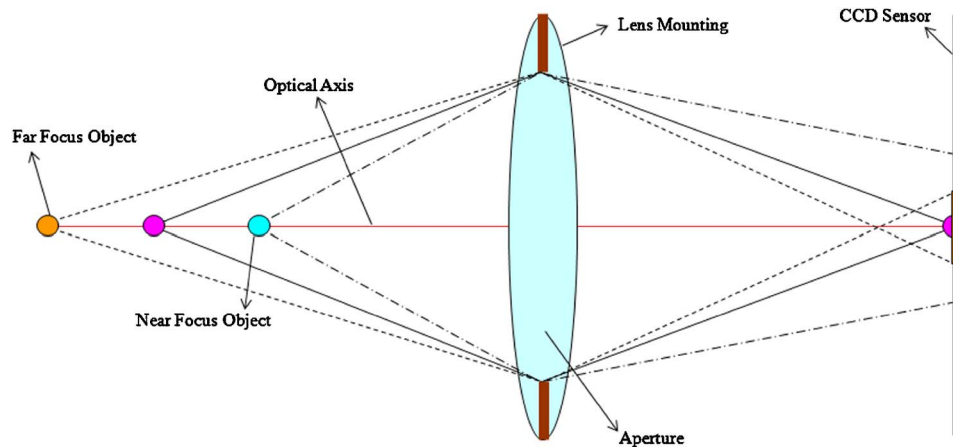


Figure 2. Representation of the schematic of the (a) wave front coding system, (b) proposed FA system.

Table 1. Comparison of conventional AF systems with the proposed system.

Autofocusing technique	Analysis module	Control module	Focusing accuracy	Hardware specifications
Manual	Human decision	Manual	Subject to human operation	Low shutter speed $f/2-f/8.0$
IRAF	Calculating the time of IR travel	Moving the focusing lens	High	High shutter speed $f/3.5-f/5.6$
TTLAF	Minimizing a phase difference	Moving the focusing lens	Very high under good conditions	High shutter speed $f/2-f/11$
SDAF	Calculating high frequency of image	Moving the focusing lens	Acceptable	Medium shutter speed $f/2-f/28$
FDAF	Estimating PSF, blur models	Restoration filters and fusion methods	Acceptable	NIL
Proposed method	Color channel shifting	Multiple filter aperture (FA)	Acceptable	30 to 1/4,000 sec. $f/5.6-f/22$

**Figure 3.** General single aperture model.

ing methods have focused on operation of multiple source images using wavelet or discrete cosine transformations (DCT)^{8,9} with *a priori* obtained camera PSF. Other methods use pyramid-based representation to decompose the source images into different spatial scales and orientations.^{10,11} Similar results, although with more artifacts and less visual stability, can be achieved by using a set of basis functions.¹² Another technique similar to pyramid representation approach has been based on wavelet transform to decompose the image into various subbands.^{13,14} The output is generated by selecting one of the decomposed subbands such that the selected subband has maximum energy. Restoration-based techniques have been carried out to overcome the out-of-focus problem. However, restoration of images with different depth of fields tend to cause reblurring and ringing artifacts in the region with low depth of field or in-focus regions.^{15,16} Even with equal depth of field the nature of restoration poses a serious limitation to the visual quality of the restored images. Another drawback is the slow convergence process of the iterative framework.

The main contribution of the proposed method is listed below:

- Multiple apertures and corresponding sensors can enhance depth information.
- Focusing process is inherently designed in accordance with color information.
- Neither image restoration nor blur identification is necessary.

- Set of images with multiple apertures and focus settings can be generated using a single image with channel shifting.
- Fusion algorithm involves separate feature-based fusion and color blending consistency to preserve the channel dependencies.
- Proposed algorithm does not need transformation or convolution operations.

Recently, images obtained at different shutter speeds were combined into an image in which full dynamic range is preserved.¹⁷ The proposed approach extends and generalizes the standard fusion approach to color images. The proposed approach does not need multiple source images captured at different aperture settings. Instead we derive different source images from a single out-of-focus image to obtain various positions of focal points.^{18–20} For each focal point three color channels are aligned and the corresponding images are used for fusion.

MULTIPLE FILTER-APERTURE (FA) MODEL

An aperture of a lens can adjust the amount of incoming light accepted through the lens. It can also control the focal length, camera-to-object distance, and depth of field. Generally, the center of an aperture is aligned on the optical axis of the lens. Any controlled aperture accepts light from various angles depending on the object position. Correspondingly, the convergence pattern on the imaging plane forms either a point or a circular region as shown in Figure 3. For

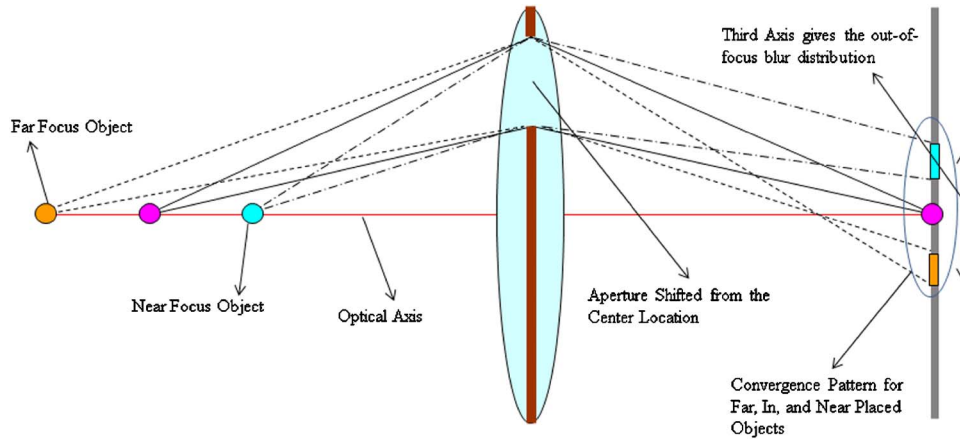


Figure 4. Aperture shifted from the center.

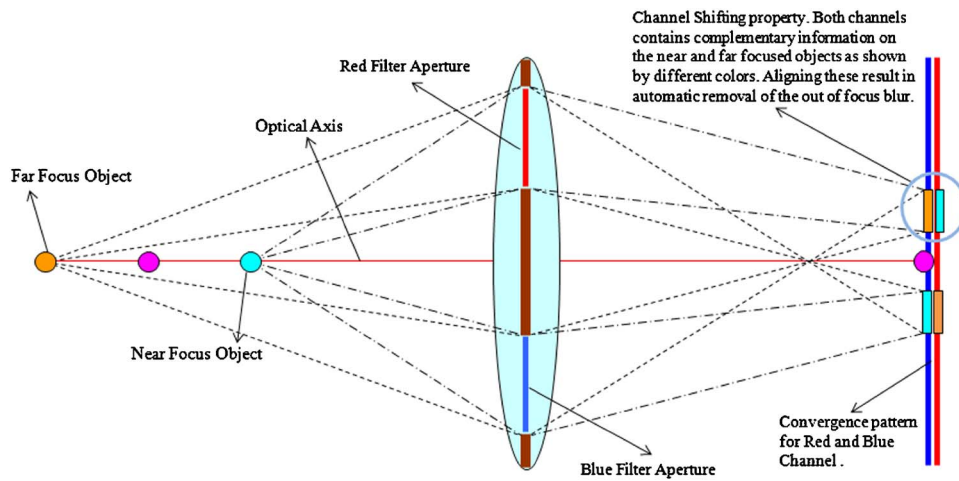


Figure 5. Multiple aperture setup for red and blue channel filters.

objects placed at near-, mid-, and far-focal distance the image convergence takes place either in front, on, or behind the CCD/CMOS sensor. However, this image convergence as well as the blur information can only be represented in a bi-axial plane as shown in Fig. 3.

An interesting alternative for tri-axial representation of the image and out-of-focus blur was found to be achieved using non-centric aperture as shown in Figure 4. For a non-centric aperture located either on the upper or lower part of the optical axis, the convergence pattern was found to be split between these axes. The split difference between the patterns will give another dimension to the conventional bi-axial plane making it a tri-axial representation. For the objects at the same positions (near, in, far focal distances), the convergence pattern of the channel aperture form an overlapping convergence on the CCD/CMOS sensor. For instance, the near focal distance object converges on the upper part of the optical axis where, at the same position, the far focal distance object converges on the lower part. If these overlapping channels are exactly aligned, then we will have a focused pattern in the image.

An extension of the above approach will be to use a lens with two apertures on either side of the optical axis. An

interesting phenomenon that can be observed is that, for the near and far focused objects, the convergence pattern lies on opposite sides for each aperture in reverse order for each channel. For example, the red aperture can have near-focused convergence on the top and far-focused convergence on the bottom whereas the blue aperture has far-focused convergence on the top and near-focused convergence at the bottom, as shown in Figure 5. This phenomenon is called the filter-aperture (FA) extraction. The out-of-focus blur is now distributed among the color channels forming the image.

Now we extend the above multiple aperture convergence to a typical RGB image scenario. To obtain an RGB image using the multiple aperture configurations we need to obtain R, G, and B channel convergence patterns separately. This can be done using three apertures in a Bayer pattern where the images are individually obtained on the sensor for the three apertures and later combined to form the RGB image. Evidently, multiple apertures provide additional depth information of objects at different distances. Since any color image is composed of three channels, we have used three apertures and, correspondingly, three filters (see Figure 6).

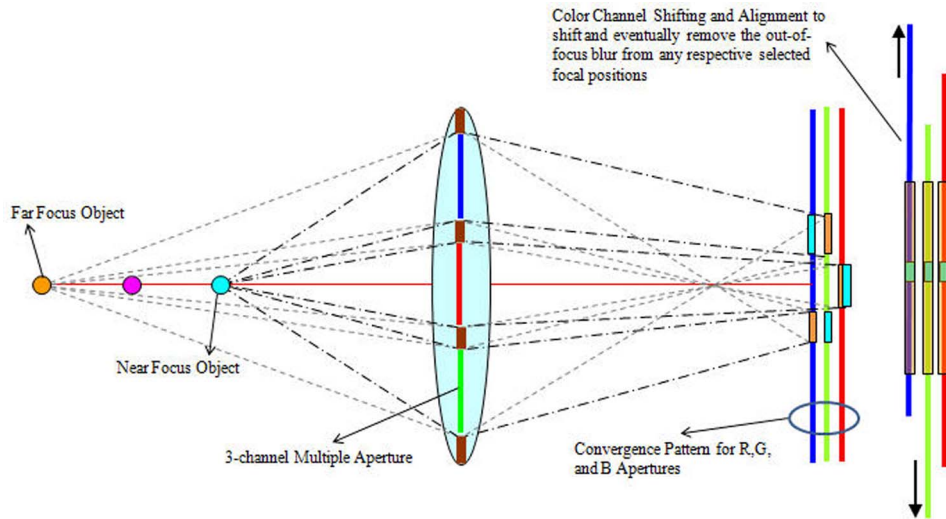


Figure 6. Multiple FA model showing the convergence pattern for the R, G, and B color channels.

The main advantage of the FA model is that it can provide an alternative method for blur estimation in autofocusing applications. Images acquired by using a normal lens have uniform or spatially variant blur confined on all channels. However, in the proposed algorithm, by using three filtered sensors the autofocusing problem turns into the alignment of R, G, and B channels with various depths of field. The out-of-focusing phenomenon with single and multiple aperture lenses are compared in Figure 7. As shown in Fig. 7(b) the out of focus blur is modeled as a misalignment of three color channels of R, G, and B.

DIGITAL AUTOFOCUSING ALGORITHM

The proposed algorithm uses the image obtained from the multiple FA configurations for the autofocusing application.

The proposed autofocusing algorithm consists of the following procedures to obtain a well-restored image: (i) salient feature computation, (ii) color channel shifting and alignment for selected pixels, and (iii) soft decision fusion and blending.

Salient Focus Measure

The feature saliency computation process contains a family of functions that estimate saliency information. In practice, these functions can operate on individual pixels or on a local region of pixels. When combining images having different focus measures, for instance, a desirable saliency measure would provide a quantitative measure that increases when features are better focused. Various saliency measures, including variance and gradients, have been employed and

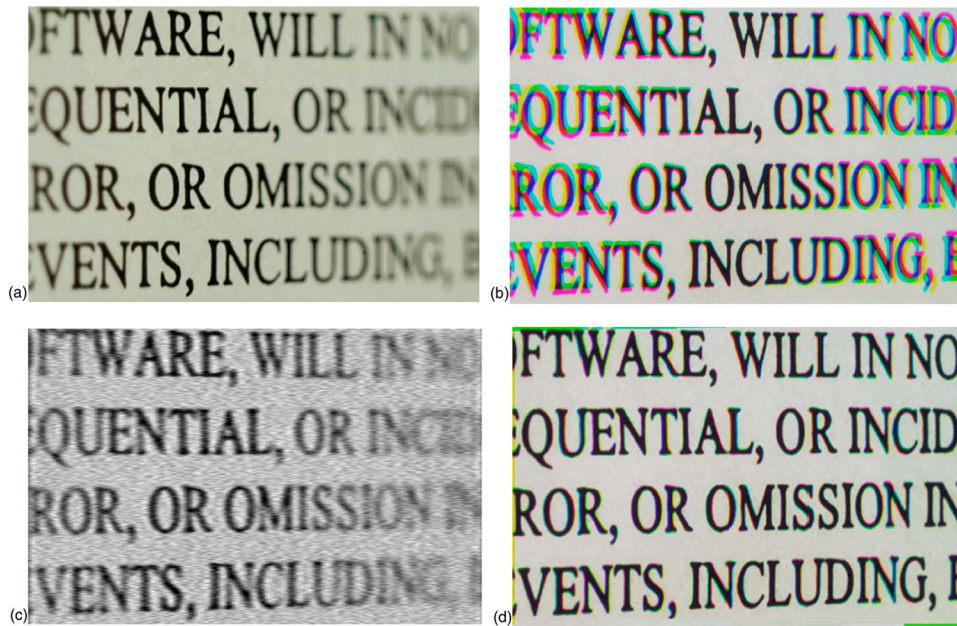


Figure 7. Comparison of out-of-focus blurs for a single aperture model and the proposed multiple aperture models: (a) and (b) out-of-focus image captured using ordinary camera and proposed FA system under same focal settings, (c) restored result using the regularized restoration method, (d) restored result using the proposed channel shifting and fusion algorithm.

validated for related applications. The saliency function only selects the frequencies in the focused image that will be attenuated due to defocusing. One way to detect a high frequency component is to apply the following absolute Laplacian operator as

$$\nabla^2 L_k = \left| \frac{\partial^2 L_k}{\partial x^2} \right| + \left| \frac{\partial^2 L_k}{\partial y^2} \right|. \quad (1)$$

The second derivatives in the x and y directions often have opposite signs and tend to cancel each other. In the case of textured images, this phenomenon may frequently occur and the Laplacian behaves in an unstable manner. However, this problem can be overcome by using the absolute Laplacian as in Eq. (1). In order to accommodate for possible variations in the size of texture elements, we compute the partial derivative using a variable spacing between pixels for computing the derivatives. Hence a discrete approximation to the modified Laplacian, $ML_k(i, j)$, for pixel intensity, $I(i, j)$, is given as

$$ML_k(i, j) = |2I(i, j) - I(i - 1, j) - I(i + 1, j)| \\ + |2I(i, j) - I(i, j - 1) - I(i, j + 1)|. \quad (2)$$

Finally, the focus measure at a point (i, j) is computed as the sum of modified Laplacian values, in a small window around (i, j) , that are greater than a prespecified threshold value,

$$f(i, j) = \sum_{p=i-N}^{i+N} \sum_{q=j-N}^{j+N} ML_k(p, q) \text{ for } ML_k(p, q) \geq T_1. \quad (3)$$

The heuristically determined threshold value T_1 in the range 40–60 provides acceptable results in most cases. The parameter N represents the window size for computing the focus measure. In contrast to region-based autofocusing methods, we typically use a smaller window of size, e.g., $N=1$. Equation (3) can be referred to as sum modified Laplacian (SML) which is used as an intermediate image estimate for determining focus information.

Color Channel Shift and Alignment

For shifting and aligning color channels we need to find the optimal pixel-of-interest at different positions in the image according to their focal measures. These pixels-of-interest can be referred to as a focal point pixels. The term ‘‘focal point pixel’’ refers to a pixel-of-interest around which channel shifting and alignment is carried out. For a given image, the SML measure can be used to determine the focal point region whose focal measure is significantly lower than other regions of the image. Then for a given region, we select the focal point pixel either from the center of region or the pixel with the lowest focus measure. Similar operations can be performed for different selected focal point regions in different neighborhood. Henceforth, for a corresponding focal point pixel, we perform channel alignment and remove the out-of-focus blur in that given neighborhood (see Figure 8).

For a given particular image captured by using FA configuration, the out-of-focus blur was just confined to chan-

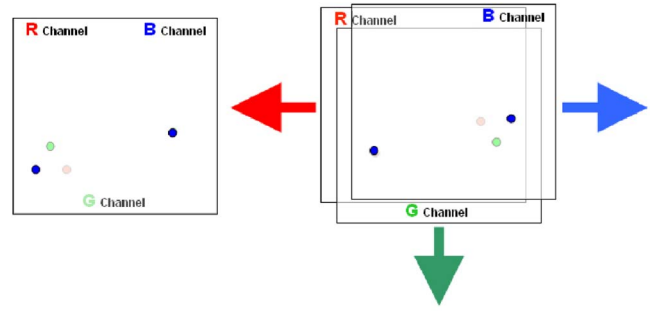


Figure 8. Schematic of channel alignment procedure for R, G, and B channels.

nels on either side of the green channel as shown in Figure 9. As can be seen from the figure, the green channel suffers minimal blur distortion as the sensor was placed at the center whereas the red and the blue channels have maximal blur distortion. The proposed autofocusing technique uses the green channel as the reference and aligns the red and the blue channels to the green channel for any particular location, such as

$$I_{\text{RGB}} = S_{(r,c)}(I_{\text{R}} + I_{\text{B}}) + I_{\text{G}}, \quad (4)$$

where $S_{(r,c)}$ represents the shift operator and the shift vector (r, c) represents the amount of shift in row and column directions for the respective red and blue channels with respect to the reference focal point on the green channel. If the shift vectors are not identical, we can generalize the above equation as

$$I_{\text{RGB}} = S(I_{\text{R}}(r_1, c_1) + I_{\text{B}}(r_2, c_2)) + I_{\text{G}}. \quad (5)$$

The shift vectors on the same sensor filter are linearly dependent. For a particular reference channel it is possible to estimate the exact number of shift vectors using the sensor filter configurations. For example, in our experiments the green channel has been used as reference, hence the red and blue pixels are misaligned by a pattern corresponding to the sensor filter as shown in Figure 10.

Soft Decision Fusion and Blending

In order to merge images with multiple focal point planes, image fusion is required on multiple channel images. Unfortunately, when the channel-shifted images are directly fused, misalignment or misregistration is unavoidable. The pixels of different channel aligned images, when fused together, may sometimes tend to overlap or get missed because of the channel shifting. This problem can be overcome by applying an inverse shift operation to the images with respect to a reference image. The reference image has to be chosen from one of the several channel shifted images extracted using channel shifting and alignment. In the proposed approach we choose the reference image as the one that will have a focal point located approximately in the center of the image,

$$I_k = S_{(r,c \in I_r)}^{-1}(I_k, I_r), \quad (6)$$

where I_r represents the reference image for registration and S^{-1} represents the inverse shift operation. After selection of

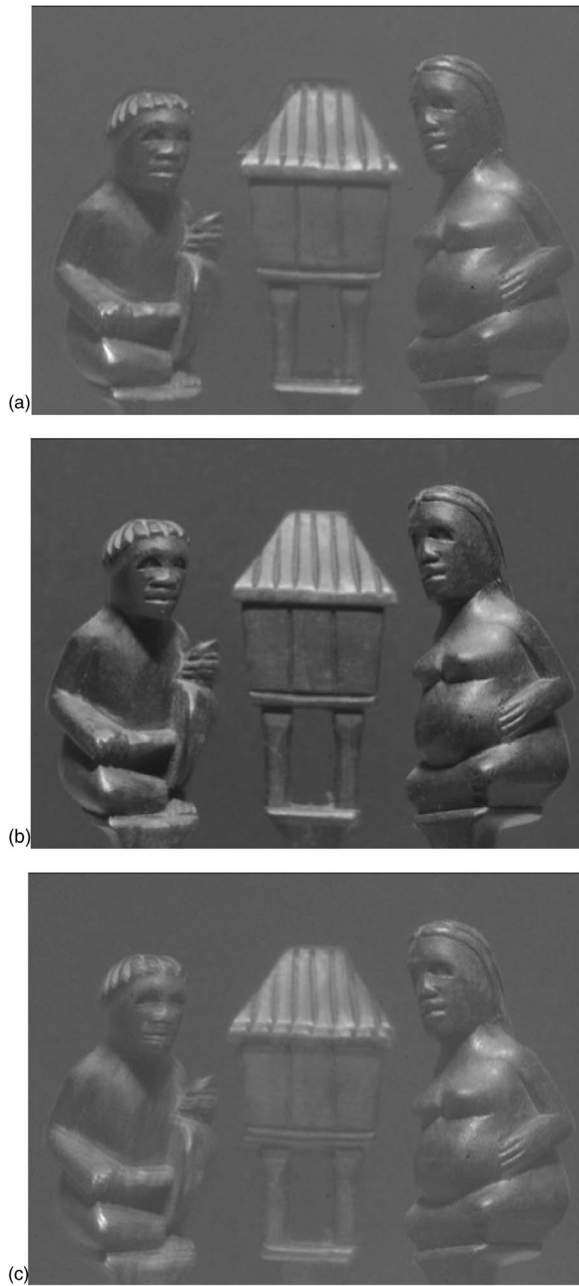


Figure 9. Multiple FA model image: (a) R, (b) G, and (c) B channels, respectively.

the focal point using the SML operator and channel alignment by channel shifting, the appropriate regions need to be selected from the given image. Given the location of the pixel-of-interest for channel alignment, we simply select an approximate region area that is defined on its neighborhood. But for a more efficient fusion process we could isolate the region around that pixel using neighborhood connectivity. For a given pixel-of-interest and the eight-neighborhood connectivity, we can extract the region more accurately for the purpose of image fusion as

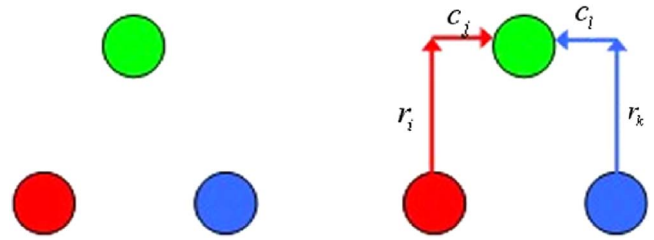


Figure 10. Row and column shift vectors for color channel shifting and alignment with reference G channel.

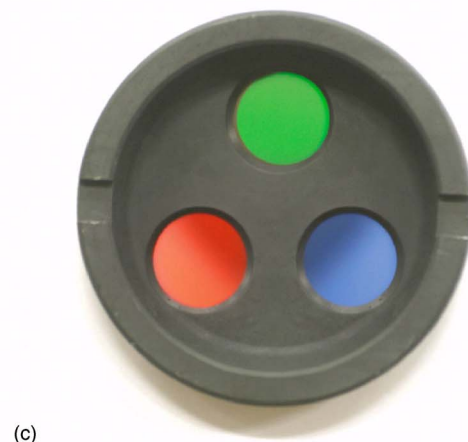
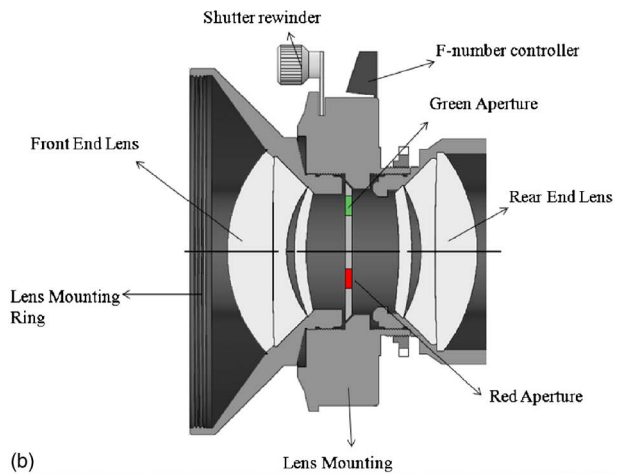


Figure 11. Experimental set up: (a) digital camera with the FA model; (b) interior configuration of the FA; and (c) the R, G, and B sensor filters.

Table II. A sample set of shift vectors estimated for different locations.

Region	Red channel (r, c)	Blue channel (r, c)
R_1 (upper left)	(10,4)	(8,5)
R_2 (upper middle)	(7,6)	(8,5)
R_3 (upper right)	(10,5)	(7,6)
R_4 (center left)	(9,4)	(10,5)
R_5 (center middle)	(9,3)	(9,3)
R_6 (center right)	(8,6)	(10,2)
R_7 (lower left)	(10,4)	(9,4)
R_8 (lower middle)	(11,6)	(9,4)
R_9 (lower right)	(11,5)	(8,3)

$$F_k = \sum_{x=i-N}^{i+N} \sum_{y=j-N}^{j+N} f_p(x|s_p, \dots, s_{i+k}, y|t_p, \dots, t_{j+k}), \quad (7)$$

where F_k represents the region around the p th focal point pixel, f_p and (s, t) represent the neighborhood connectivity.

Even though the SML operator can provide an accurate measure, we need to extract the specific region from the

Table III. Hardware configuration for the multiple FA system.

Hardware title	Specifications
Digital camera	Nikon D-100
R, G, B filters	Green-Kodak-Wratten Filter No. 58 Blue-Kodak-Wratten Filter No. 47 Red-Kodak-Wratten Filter No. 25
Focusing	APO-Symmar-L-150-5.6, 11, 22 f-5.6, f-11, f-22
Sensor	23.7 × 15.6 mm RGB CCD; 6.31 million total pixels
Lens mounting	Schneider Apo-Tele-Xenar Relative aperture focal length -5.6/250
Shutter speed	30 to 1/4,000 sec. and bulb
Color mode	Triple mode for R, G, and B channels

image for fusion. One of disadvantages of the FA model is that, for the channel-aligned images with closely located focal points, the SML operator does not always perform well. Hence, we used a color-based region segmentation algorithm for extracting selective regions from the channel-

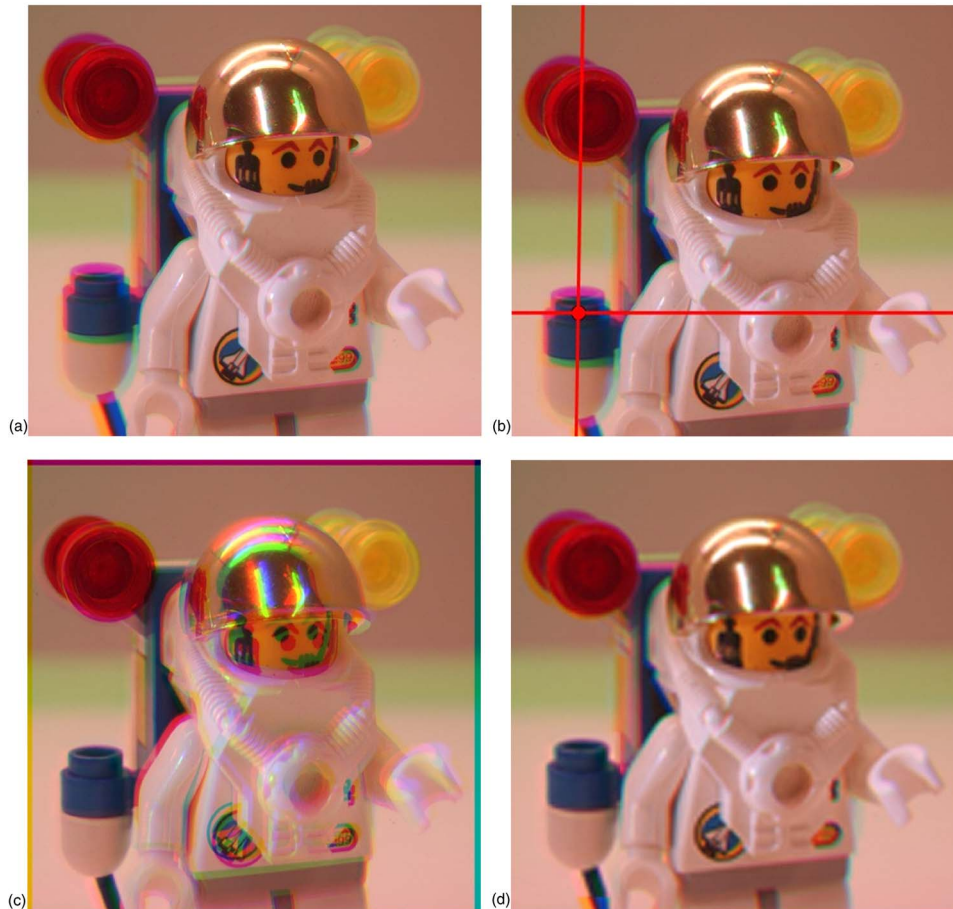


Figure 12. Experimental results: (a) the source image; (b) the focal point location for channel shifting and alignment; (c) the image after channel shifting to new focal point location; and (d) the final image fused from (a) and (c).

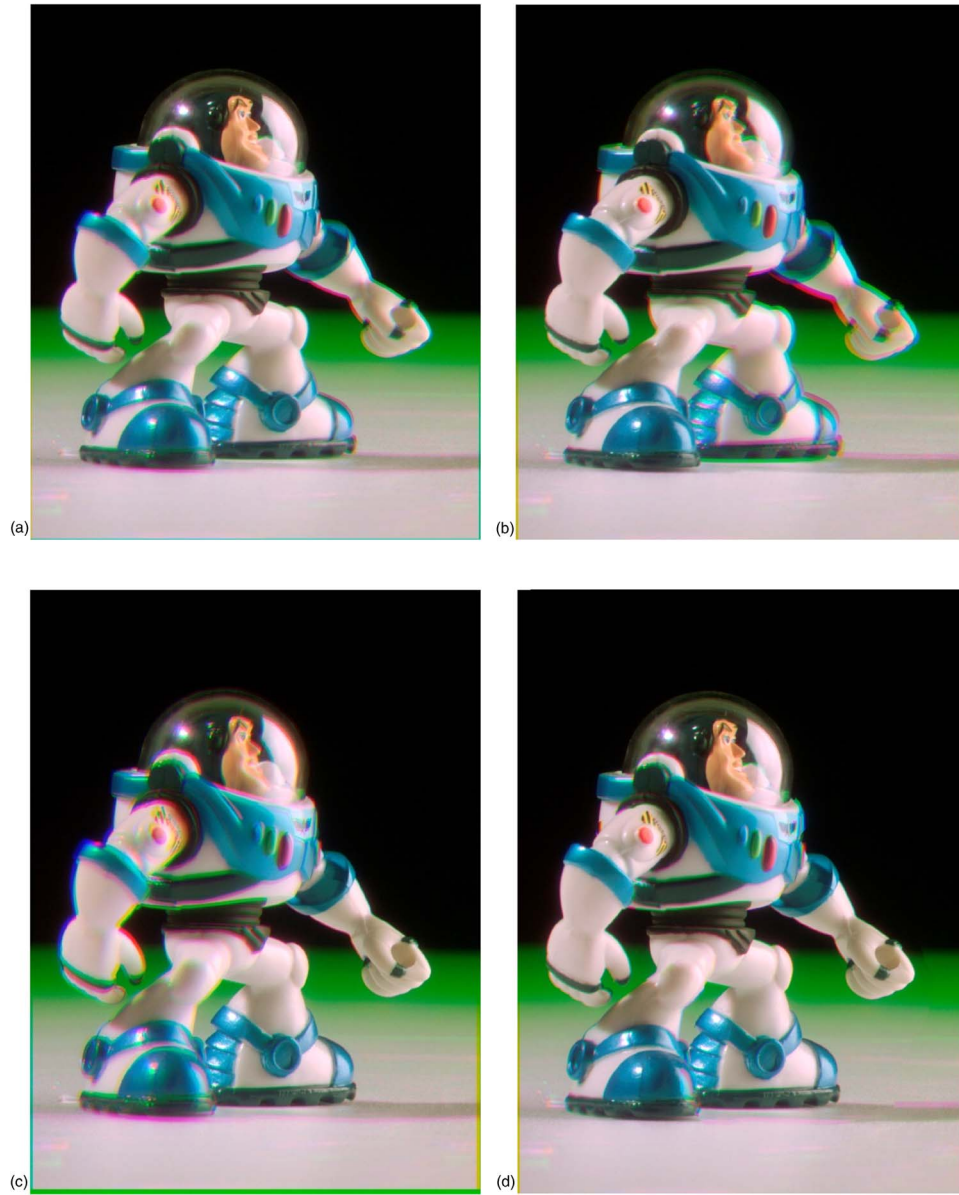


Figure 13. Experimental results: (a) the source image; (b) objects closer to the left side of the image are focused and object to the right side are outoffocus; (c) similar set up with the focus on the right side; and (d) the final image fused from (b) and (c).

aligned images if the SML results are not good enough. When fusing color images, features such as edge and textures should be preserved, and also the color blending consistency should be maintained. The fusion process is performed on each level of the channel-aligned images in conjunction with SML to generate the composite image C. The reconstruction process integrates information from different levels as

$$I_{ck} = F_k \cdot I_{ak} + (1 - F_k)I_{bk} \quad (8)$$

and

$$I_a = S_{(r,c \in I_r)}^{-1}(I_a, I_r), \quad (9)$$

where I_{ck} represents the reconstructed image from two input images I_{ak} and I_{bk} . The variable k represents the regions extracted based on their respective focal measure. The inverse shifting operation is described in Eq. (9) where I_r represents the reference image and $(r, c \in I_r)$ the corresponding shift vectors with respect to I_r . A typical problem of image fusion is the appearance of unnatural borders between the different decisions regions due to overlapping blur at focus boundaries. To combat this, soft decision blending can be employed using smoothing or low pass filtering of the saliency parameter F_k . In this paper Gaussian smoothing has been used to obtain the desired effect of blending. This creates weighted decision regions where a linear combination of pixels in the two images A and B are used to generate corresponding pixels in the fused image C. We then have

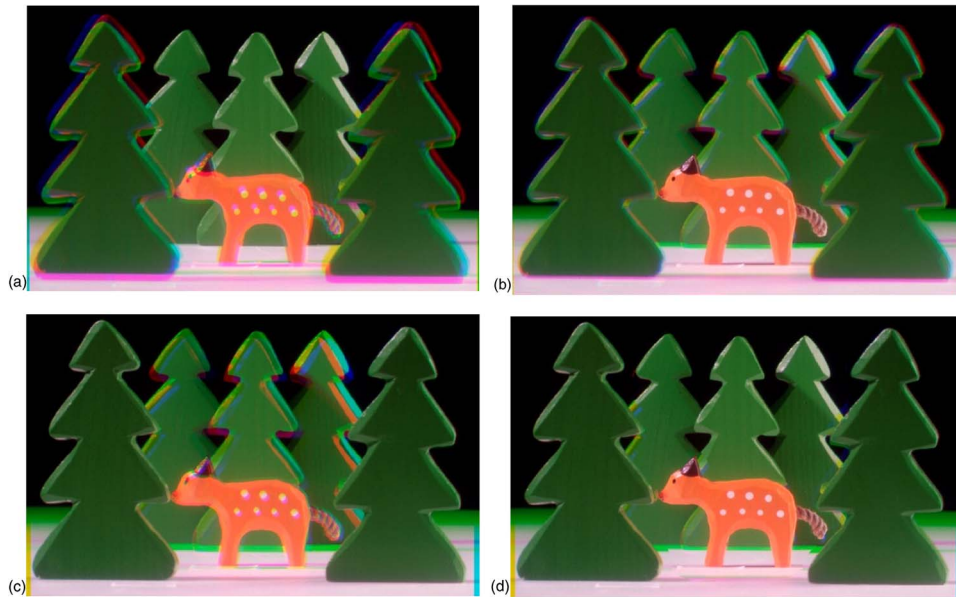


Figure 14. Experimental results: (a) the source image; (b)–(c) channel shifted images for focal points at near and center positions; and (d) the final image obtained by fusing (a)–(c).

$$I_{ck} = \tilde{F}_k \cdot I_{ak} + (1 - \tilde{F}_k)I_{bk}, \quad (10)$$

where \tilde{F}_k is now a smoothed version of its former self. At times there can be missing pixels in the fused image which are not selected using the SML. The number of missing pixels varies from image to image, but is always confined to a very small portion of the entire image. The missing pixels have to be replaced with pixels from any one of the available channel aligned images. One simple way to find an appropriate replacement is to get the location of the missing pixel in the image and then match it with the image whose focal point pixel is nearest to the respective missing pixel:

$$I(x, y) = \min \text{dis}\{I(x, y), f_p(x, y)\}. \quad (11)$$

EXPERIMENTAL RESULTS

Dataset Simulation and Experiments

In order to demonstrate the performance of the proposed algorithm, we used test images captured using the proposed

multiple FA model with multiple out-of-focus objects in the background. The experimental setup is shown in Figure 11 which represents the camera used for the experiments along with the multiple FA configurations of the camera and the sensor filter. The hardware specifications used for the system are listed in Table III. Experiments were performed on an RGB image of size 640×480 . Here, each image contains multiple objects at different distances from the camera. Figure 12(a) represents a test image with low depth-of-field, where focus is on the objects close to the camera lens. The channels aligned for the focal point are shown in Fig. 12(b). The image after channel shifting is shown in Fig. 12(c). The blue object in the back of the astronaut was out of focus in Fig. 12(a), which is now in-focus in Fig. 12(c), whereas the other regions of the image tend to get defocused. The fused image of Figs. 12(a) and 12(c) is shown in Fig. 12(d). Similar results with multiple objects are shown in Figures 13 and 14. The selected focal point for the channel alignment and shifting are represented in Figures 15(f) and 15(g).

Table IV. Image quality comparisons for the various autofocusing methods.

Autofocusing method	Prior information	Mode	Input frames	Operation	RMSE	PSNR
Wiener filter	PSF	Gray	1	Pixel based	12.35	23.36
Iterative filter	NIL	Gray	1	Pixel based	8.56	26.32
Constrained least square filter	Edge	Gray	1	Pixel based	9.56	25.10
Pyramid fusion	NIL	Gray, Color	At least 2	Window based and Pixel based	5.68	28.42
Wavelet fusion	NIL	Gray, Color	At least 2	Window based and Pixel based	5.02	29.95
Proposed	NIL	Color	1	Window based and Pixel based	8.06	26.41

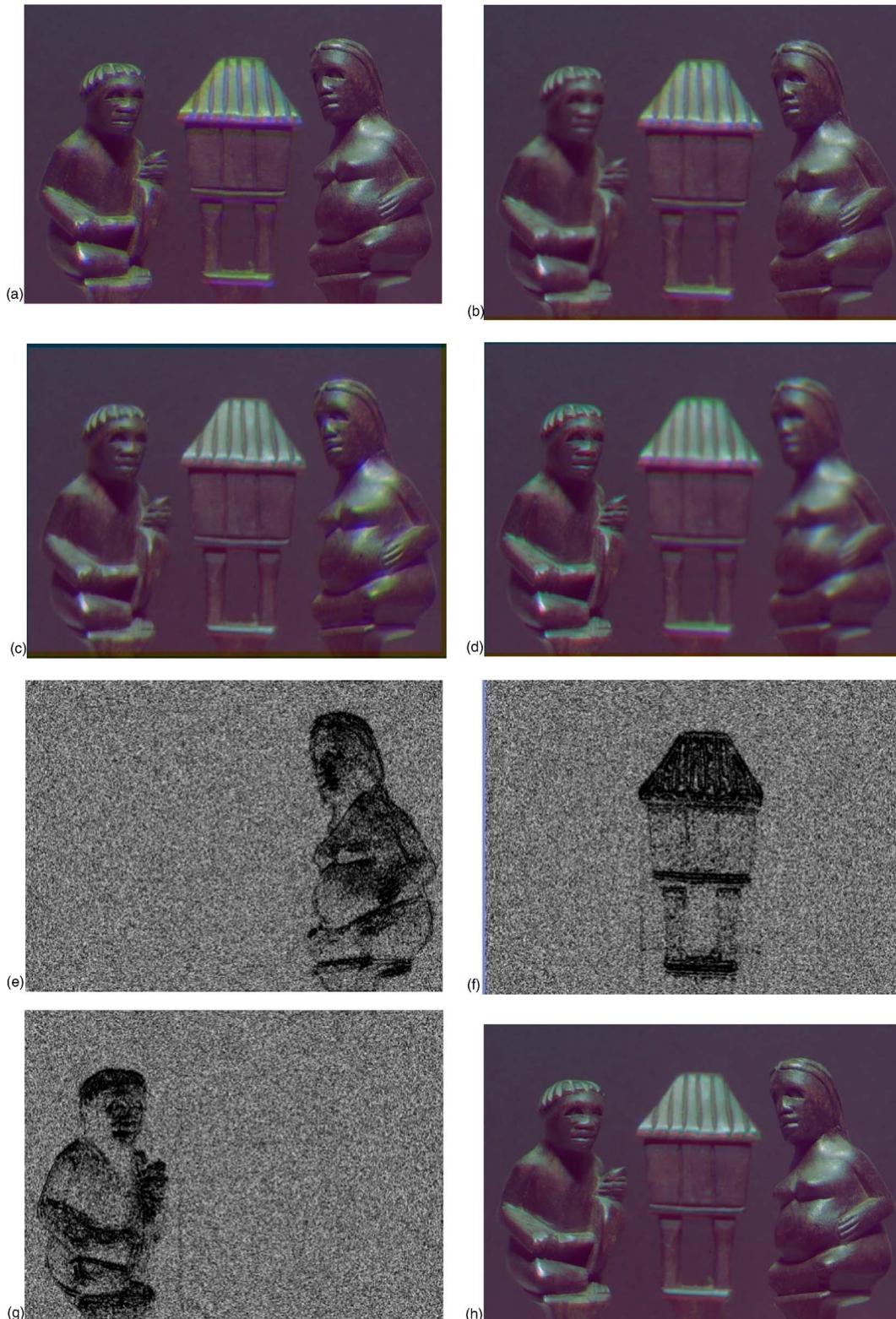


Figure 15. Experimental results: (a) the source image; (b)–(d) channel shifted images for focal points in right, center, and left positions; (e)–(g) the SML results for selected regions; and (h) the final image obtained fusing (b)–(d).

Figures 15(b)–15(d) illustrate the results of SML operator for a selected region. These figures represent images which have different out-of-focus regions obtained from single source images using channel shifting. Figure 15(e) represents

the fused image from Figs. 15(b)–15(d). The resulting fused image contains in-focus regions from respective images. The above set of results illustrates the feasibility of the proposed fusion based algorithm for autofocusing.

Performance Comparison

For measuring the performance of the multiple FA configurations, various test images were captured using the proposed system as well as the ordinary Nikon D-100 camera. The test images were then processed for out-of-focus removal using the proposed channel shifting and fusion algorithm and the ordinary camera images were restored using some state of the art restoration methods, including Wiener filter, regularized iterative restoration, constrained least squares filter, as well as some existing fusion-based methods including pyramid decomposition and wavelet methods. The performance metric in the form of PSNR and RMSE were obtained for the test images using the above algorithms as given in Table IV. As can be seen in the table, the images captured using the multiple FA configurations tend to have some degradation when compared to conventional camera images when there is no out-of-focus blurs. But with the out-of-focus blur the image quality of the conventional camera images tend to drastically reduce due to processing by restoration and is more or less comparable with the restored images using the color channel shifting and fusion. However, the fusion methods tend to give slightly higher image quality, but they require multiple source input images for achieving good performance, whereas the proposed method can achieve it with just a single source input image making our method more suitable and efficient for increasing potential applications.

For aligning the blue channel with the green channel the pixels have to be shifted in an upward direction and towards the left or diagonally to the left and vice versa for the red channel. In our experiments we tried precomputing the shift vectors at nine different locations on a test image manually using the above convention. We found that the shift vectors differ slightly for different regions on the image, as shown in Table II. These shift vectors were then used accordingly for various test images based on the location of the focal point pixel in one of the nine regions. The corresponding shift vectors were then used to align the channels.

CONCLUSIONS

In this paper, we proposed an autofocusing algorithm which restores an out-of-focus image with multiple, differently out-of-focus objects. A novel FA configuration is proposed for modeling out-of-focus blur in images. The proposed algorithm starts with a single input image and multiple source images with different apertures are generated using channel shifting. The fusion is carried out for segmented regions from each source image using the SML operator. The soft decision fusion algorithm overcomes undesired artifacts in the region of merging in the fused images. Experimental results show that the proposed algorithm works well for the images with multiple out-of-focus objects.

ACKNOWLEDGMENTS

This research was supported by Seoul Future Contents Convergence (SFCC) Cluster established by Seoul R&BD Program and by the Korea Science and Engineering Foundation (KOSEF) through the National Research Laboratory Program funded by the Ministry of Science and Technology (M103 0000 0311-06J0000-31110).

REFERENCES

- ¹Y. Ishihara and K. Tanigaki, "A high photosensitivity IL-CCD image sensor with monolithic resin lens array", in *Proc. IEEE Integrated Electronic and Digital Microscopy* (IEEE Press, Piscataway, NJ, 1983) pp. 497–500.
- ²J. Tanida, R. Shogenji, Y. Kitumara, K. Yamada, M. Miyamoto, and S. Miyatake, "Color image with an integrated compound imaging system", *Opt. Express* **18**, 2109–2117 (2003).
- ³E. R. Dowski and G. E. Johnson, "Wavefront coding system: a modern method of achieving high performance and/or low cost imaging systems", *Proc. SPIE* **3779**, 137–145 (1999).
- ⁴S. Kim and J. K. Paik, "Out-of-focus blur estimation and restoration for digital autofocusing system", *Electron. Lett.* **34**, 1217–1219 (1998).
- ⁵J. Shin, V. Maik, J. Lee, and J. Paik, "Multi-object digital autofocusing using image fusion", *Lect. Notes Comput. Sci.* **3708**, 806–813 (2005).
- ⁶V. Maik, J. Shin, and J. Paik, "Regularized image restoration by means of fusion for digital autofocusing", *Lecture Notes in Artificial Intelligence* **3802**, 929–934 (2005).
- ⁷G. Lighthart and F. Groen, "A comparison of different autofocus algorithms", *IEEE Int. Conf. Pattern Recognition* (IEEE Press, Piscataway, NJ, 1992) pp. 597–600.
- ⁸M. Subbarao, T. C. Wei, and G. Surya, "Focused image recovery from two defocused images recorded with different camera settings", *IEEE Trans. Image Process.* **4**, 1613–1628 (1995).
- ⁹M. Matsuyama, Y. Tanji, and M. Tanka, "Enhancing the ability of NAS-RIF algorithm for blind image deconvolution", *Proc. IEEE Int. Conf. Circuits and Systems*, vol. 4 (IEEE Press, Piscataway, NJ, 2000) pp. 553–556.
- ¹⁰A. Tekalp and H. Kaufman, "On statistical identification of a class of linear space-invariant image blurs using non minimum-phase ARMA models", *IEEE Trans. Acoust., Speech, Signal Process.* **ASSP36**, 1360–1363 (1988).
- ¹¹K. Kodama, H. Mo, and A. Kubota, "All-in-focus image generation by merging multiple differently focused images in three-dimensional frequency domain", *Lect. Notes Comput. Sci.* **3768**, 303–314 (2005).
- ¹²K. Aizawa, K. Kodama, and A. Kubota, "Producing object-based special effects by fusing multiple differently focused images", *IEEE Trans. Circuits Syst. Video Technol.* **10**, 323–330 (2000).
- ¹³L. Bogoni and M. Hansen, "Pattern selective color image fusion", *Int. J. Pattern Recognit. Artif. Intell.* **34**, 1515–1526 (2001).
- ¹⁴S. Li, J. T. Kwok, and Y. Wang, "Combination of images with diverse focuses using the spatial frequency", *Int. J. Inf. Fusion* **2**, 169–176 (2001).
- ¹⁵Z. Zhang and R. S. Blum, "A categorization of multiscale-decomposition-based image fusion schemes with a performance study for a digital camera application", *Proc. IEEE* **87**, 1315–1326 (1999).
- ¹⁶V. Maik, J. Shin, J. Lee, and J. Paik, "Pattern selective image fusion for multi-focus image reconstruction", *Lect. Notes Comput. Sci.* **3691**, 677–684 (2005).
- ¹⁷A. Kubota, K. Kodama, and K. Aizawa, "Registration and blur estimation method for multiple differently focused images", *Proc. IEEE Int. Conf. Image Processing*, vol. 2 (IEEE Press, Piscataway, NJ, 1999) pp. 515–519.
- ¹⁸S. K. Lee, S. H. Lee, and J. S. Choi, "Depth measurement using frequency analysis with an active projection", *Proc. IEEE Conf. Image Processing*, vol. 3 (IEEE Press, Piscataway, NJ, 1999) 906–909.
- ¹⁹G. Piella, "A general framework for multi resolution image fusion: From pixels to regions", *J. Inf. Fusion* **4**, 259–280 (2003).
- ²⁰T. Adelson and J. Y. Wang, "Single lens stereo with a plenoptic camera", *IEEE Trans. Pattern Anal. Mach. Intell.* **2**, 99–106 (1992).